Computational Simulation of Penetrating Trauma in Biological Soft Tissues using the Material Point Method

Irina IONESCU*[+], James GUILKEY*[++], Martin BERZINS*[‡],
Robert M. KIRBY*[‡], Jeffrey WEISS*[+]
**Scientific Computing and Imaging Institute,*
Departments of [+]Bioengineering, [++]Mechanical Engineering,
and [‡]School of Computing, University of Utah

Abstract. The objective of this research was to develop realistic computational models for soft tissues subjected to finite deformation and failure, and to test these models in the context of numerical simulations of penetrating trauma injuries. A transversely isotropic hyperelastic model with strain-based failure criteria was used to represent the behavior of anisotropic soft tissue. The constitutive model was implemented into an existing numerical code based on the Material Point Method (MPM). The penetration of a low-speed bullet through a myocardium material slab was simulated and several wounding scenarios were analyzed and compared. The material symmetry, the type of contact modeled between the bullet and the soft tissue and the bullet speed were shown to have a significant influence on the wound profile.

1. Introduction

Injuries due to penetrating trauma from bullet or knife wounds represent a significant healthcare problem [1]. An improved understanding of the factors that control the extent of tissue damage from these wounds can provide the means to improve diagnosis and treatment. Soft tissue failure (skeletal and cardiac muscle, ligament and tendon, nerve) typically represents a large part of the damage resulting from penetrating trauma [2]. However, the detailed three dimensional prediction of soft tissue failure is complicated by the highly anisotropic nature of the materials as well as the lack of appropriate failure models.

The objective of this research was to develop realistic computational models for soft tissues subjected to finite deformation and failure and to implement and test these models in the context of numerical simulations of penetrating trauma injuries.

2. Methods

The current research focused on modeling penetrating injuries to an analog of the myocardium. A “two-surface” strain-based failure criterion was incorporated into a hyperelastic constitutive model of the myocardium. The myocardium was represented as a composite of matrix and collagen fibers, each failing by different strain-driven failure mechanisms. Bullet penetration simulations of myocardial material slabs were performed using the Material Point Method (MPM) with explicit time integration [3].

2.1 Constitutive model and Failure Criteria

A strain-based failure model was developed for transversely isotropic hyperelastic soft tissues. The myocardium was modeled as a transversely isotropic hyperelastic material, comprised of an isotropic Mooney-Rivlin matrix reinforced by a single fiber family [4]. The local fiber direction was described by a unit vector $\mathbf{a^0}$ that changes direction and length as the material deforms, so that:

$$\boldsymbol{F} \cdot \boldsymbol{a}^0 = \lambda \boldsymbol{a}\,, \tag{1}$$

where λ denotes the local fiber stretch and $\boldsymbol{F}$ is the deformation gradient tensor. The strain energy function W was written in terms of the matrix and fiber response, respectively:

$$W = F_1(I_1, I_2) + F_2(\lambda)\,, \tag{2}$$

where I_1 and I_2 are the first and second invariants of the right Cauchy-Green deformation tensor. The matrix was modeled using a Mooney-Rivlin model, while the elastic response of collagen fibers was considered exponential in the toe region and linear subsequently [5]:

$$\begin{aligned} &F_1(I_1, I_2) = c_1(I_1 - 3) + c_2(I_2 - 3) \\ &\lambda \frac{\partial F_2}{\partial \lambda} = \begin{cases} 0, & \lambda < 1 \\ c_3 e^{c_4(\lambda - 1))-1}, & \lambda \le \lambda^* \\ c_5 \lambda + c_6, & \lambda > \lambda^* \end{cases} \end{aligned} \tag{3}$$

The five material coefficients to define the transverse isotropy of the above described material have been chosen as follows. The Mooney-Rivlin constants for the matrix were taken as c_1 = 2.1 KPa, c_2 = 0. The elastic fibers were characterized by a constant to scale the exponential stresses in the toe region c_3 = 0.14 KPa, the rate of fiber uncrimping c_3 = 22, and the modulus of the straightened collagen c_5 = 100 Kpa [4]. The stretch at which the collagen fibers straighten was assigned a value of λ^* = 1.4 [4]. The constant c_6 was determined from the condition that the collagen stress is continuous at λ^*. The material was considered as nearly incompressible, with a bulk:shear modulus ratio of 47.62. To represent the type of material symmetry exhibited by the myocardium, the fiber direction $\mathbf{a^0}$ was varied through the thickness of the slab so that fibers rotated clockwise 180^o from epicardial to endocardial surface (Fig. 1a).

A strain-based failure criterion was developed to quantify failure resulting from the wounding. The myocardium can be seen as a composite material whose phases, matrix and fibers, have different ultimate strains, the collagen fibers withstanding a higher tensile strain than the matrix. Two modes of failure were represented: matrix failure under shear (Fig. 1b) and fiber failure under tension (Fig. 1c); hence the failure criterion was defined in terms of two failure surfaces. With these assumptions, the Cauchy stress was decomposed as:

$$\boldsymbol{\sigma} = \boldsymbol{\sigma}_{\text{volumetric}} + \boldsymbol{\sigma}_{\text{matrix}} + \boldsymbol{\sigma}_{\text{fibers}} \tag{4}$$

The matrix material was considered to fail locally if the maximum shear strain at a point exceeded 50% strain [6] and the matrix contribution to the stress was annulled:

$$\gamma_{\text{matrix}} > 50\% \quad \Rightarrow \quad \boldsymbol{\sigma}_{\text{matrix}} = 0,\ \boldsymbol{\sigma}_{\text{volumetric}} = 0 \tag{5}$$

If the fiber stretch λ exceeded 40% [5] strain at a point, the fiber was considered failed and its contribution to the total state of stress was annulled:

$$\varepsilon_{\text{fibers}} > 40\% \quad \Rightarrow \quad \boldsymbol{\sigma}_{\text{fibers}} = 0 \tag{6}$$

If both of the above conditions were fulfilled locally, the material point exhibited total failure.

At each material point, the strains in the matrix and fibers were compared with the assigned failure values. A failure flag was defined at each of the particles in the model, to record if and what particular type of material failure may occur. The type of failure and the distribution of failed particles helped to interpret the wound profile.

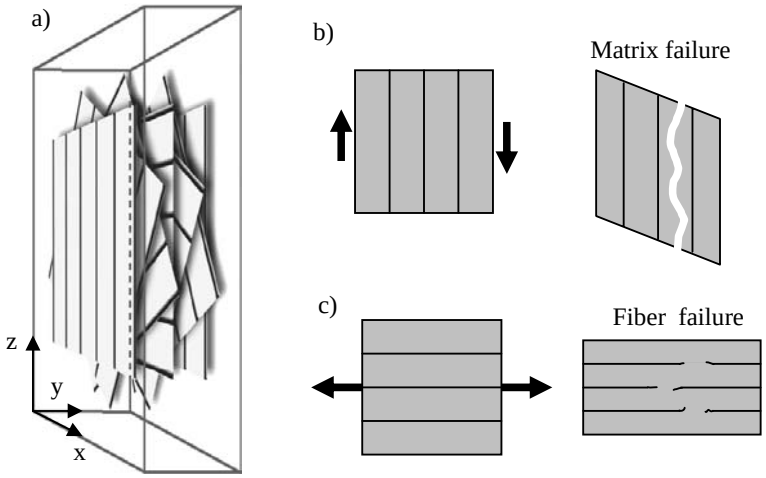

Fig. 1. a) Material symmetry of the myocardial slab. The local fiber direction rotated 180 degrees through thickness of the slab. Failure modes: b) matrix failure via shear strain and c) fiber failure via elongation along the fiber direction.

2.2 Numerical Discretization with Material Point Method

The equations of motion were discretized in space using the Material Point Method (MPM) [3]. Explicit time integration was used. MPM is a particle method for simulations in computational mechanics that is implemented within the Uintah computational framework, a software infrastructure for large-scale numerical simulations [7]. Like other quasi-meshless methods, MPM offers an attractive alternative to traditional finite element (FE) methods [8] because it simplifies the modeling of complex geometries, large deformations and fragmentations that are typical of penetrating trauma to the torso or its components.

2.3 Test problems

To test the failure model, the penetration of a bullet through a slab of myocardium was simulated. A 50×10×50 mm myocardial slab was considered (Fig. 1a). The *x*-*y* and *y*-*z* side boundaries were fixed, while the *x*-*z* faces were free of constraints. A 9 mm diameter bullet was modeled as an elastic-plastic material with neo-Hookean elastic material properties (properties used: bulk modulus K = 117 GPa, shear modulus μ = 53.8 GPa, yield stress 422.6 MPa, hardening modulus 53.8 MPa). The simulations consisted of $1.6 \cdot 10^6$ material points, distributed in a 4x4x4 spacing in each grid cell.

Simulations of a bullet wound to a myocardial tissue sample were performed using several material symmetry models and wounding scenarios. Simulations were performed for bullet velocities in the 'low-speed' range, i.e. less than 1000 ft/s. Low speed projectiles

have been shown to produce most of their damage by crushing the tissue, and almost no damage due to cavitation. Two initial bullet velocities were considered: 150 m/s and 50 m/s. To study the effects of anisotropy on wound profile, an isotropic material slab was also considered and results were compared to that obtained for the anisotropic case. Frictional contact with a coefficient of friction of 0.08 was considered between the bullet and the soft tissue. The matrix, fiber, or total tissue failure were recorded for the each of the simulations.

3. Results

The wound profile in each of the cases showed the damage from the bullet as it passed through the myocardial sample. The wound profile for the case of a bullet with an initial speed of 150 m/s and an anisotropic slab is presented in Fig. 2.

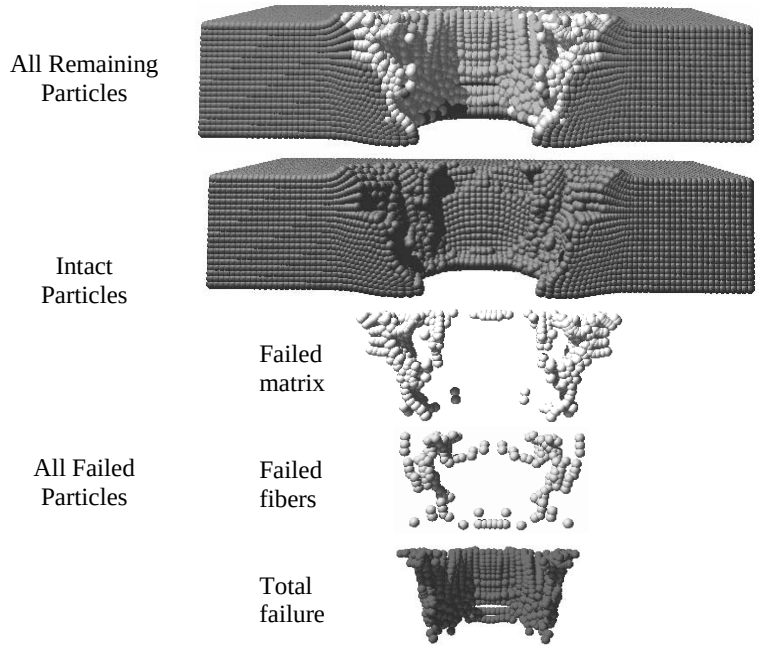

Fig. 2. Wound profile and failed particles for a myocardium slab in which material fibers rotate 180^{o} through thickness. The failed particles are separated by the type of failure undergone: matrix, fiber or total tissue failure.

In all cases the entrance wound had a clean appearance and an approximate circular shape. Total tissue failure was observed in the immediate vicinity of the bullet tract, zones of matrix and fiber failure surrounding the inner total tissue failure zone (Fig. 2). The wound tract diameter increased uniformly from entrance to exit. The exit wound appeared to be elliptic, the fiber alignment in the slab outer layer perhaps influencing its regular shape. The phenomenon of cavitation of the bullet was not observed, due primarily to the small thickness of the slab.

The wound profiles and shape of the exits wounds were different between the anisotropic and isotropic cases (Fig. 3). The shape of the exit wound was elliptic for the case of anisotropic material symmetry (Fig. 3a) and circular for the case of isotropic material symmetry (Fig. 3b).

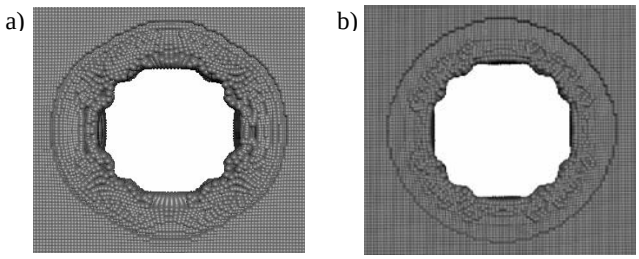

Fig. 3. Effects of anisotropy on the wound profile (exit wound view): a) anisotropic slab; b) isotropic slab (initial bullet speed 50 m/s).

4. Discussion

The results of the test problems are encouraging and can be interpreted in terms of the physics of the bullet penetration.

The wound profile (Fig. 2) showed an approximate circular central area of complete tissue disruption in the bullet path presenting a diameter increase from entrance to exit, as bullets were reported to produce [1]. The adjoining area of 'injured' soft tissue, presented a layered failed particle distribution. As the bullet penetrated the slab, it transferred its energy to the surrounding tissue producing damage. Closest to the wound tract, a layer of particles recording total tissue failure was observed, surrounded by a layer of particles with fiber failure and matrix failure. The damage dissipated with the distance from the bullet tract, as physically expected [1].

Fiber reinforcement was shown to make a difference even for very slow speeds (50 m/s) to the wound appearance (Fig. 3). The isotropic case presented a totally symmetric wound pattern, whereas in the anisotropic case the collagen fibers contribute to the asymmetry of the wound profile.

The jaggedness of the exit wound (Fig. 3) is most likely a result of projecting a circular object (the bullet) to a cartesian mesh. This artifact becomes less prominent with increasing grid resolution. Future work will investigate the use of higher order interpolation, which is also likely to improve the results.

It is understood that the predictions of failure from these simulations will clearly depend on the assumptions associated with the failure model. Future research will consider alternative myocardial material models [9] and failure properties. Beyond this, the approach of using MPM with constitutive models that explicitly represent failure in composites may be useful for large-scale simulations of injuries to the torso that affect multiple organs. Preliminary large-scale simulations of the entire torso, including bones and soft tissue organs, have yielded encouraging results. Others have reported on the use of MPM for modeling material failure and accommodating structural failure under impact [10]; this research demonstrates the feasibility of using MPM for computational modeling of soft tissue failure associated with penetrating wounds.

References

[1] Bartlett CS, *'Clinical Update: Gunshot Wound Ballistics'*: Clin Orth and Rel Research, 2003; 408:28-57

[2] Eisler RD, Chatterjee AK, Burghart GH, *'Simulation and modeling of penetrating wounds from small arms'*: Stud Health Technol Inform, 1996; 29:511-22.

[3] Sulsky D, Chen Z, Schreyer HL, *'A particle method for history dependent materials'*: Comp Meth Appl Mech Eng, 1994, 118:179-196.
[4] Humphrey JD, Strumpf RK, Yin FC, *'Determination of a constitutive relation for passive myocardium: II. Parameter estimation'*, J Biomech Eng., 1990; 112(3):340-346.
[5] Weiss JA, Maker BN, Govindjee S., *'Finite element implementation of incompressible, transversely isotropic hyperelasticity'*: Comp Meth Appl Mech Eng, 1996; 135:107-128.
[6] Hunter PJ, McCulloch AD, ter Keurs HE, *'Modelling the mechanical properties of cardiac muscl*e': Prog Biophys Mol Biol, 1998; 69:289-331.
[7] Parker S, *'A Component-based Architecture for Parallel Multi-Physics PDE Simulation'*: Intl Conf on Comp Science (ICCS2002) Workshop on PDE Software, 2002, April 21-24.
[8] Chen Z, Brannon R, *'An Evaluation of the Material Point Method'*: Sand Report, SAND2002-0482.
[9] Guccione JM, McCulloch AD, Waldman LK, *'Passive material properties of intact ventricular myocardium determined from a cylindrical model'*: J Biomech Engng, 1991; 113:42-55.
[10] Chen Z, Hu W, *'Recent Advances in First-Principle Simulation of the Transition from Continuous to Discontinuous Failure under Impact'***,** 16th Eng Mech Conf of the ASCE, Seattle, Washington, 2003, July 16-18.

Acknowledgement

This work was supported by a grant from the DARPA, executed by the U.S. Army Medical Research and Materiel Command/TATRC Cooperative Agreement, Contract # W81XWH-04-2-0012.